Accepted Version Langmuir 2024, 40, 7, 3783–3792 doi.org/10.1021/acs.langmuir.3c03641

The Relative Strength of Polycation Adsorption on Oxide Surfaces

*John Akintola,[1] Samir Abou Shaheen,[1] Qiang Wu,[2] Joseph B. Schlenoff[1]**

[1]Department of Chemistry and Biochemistry, The Florida State University

[2]Department of Industrial and Manufacturing Engineering, FAMU-FSU College of Engineering

Tallahassee, FL 32306-4390 USA

*jschlenoff@fsu.edu

Keywords: polyelectrolyte, salt, desorption, monolayer, charge regulation, polyvinylpyridine, silica

Accepted Version Langmuir 2024, 40, 7, 3783–3792 doi.org/10.1021/acs.langmuir.3c03641

Abstract

Polyelectrolyte adsorption to surfaces is widely employed in water treatment and mining. However, little is known of the *relative* interaction strengths between surfaces and polymer. This fundamental property is assumed to be dominated by electrostatics, i.e. attractive interactions between opposite charges, which are set by the overall ionic strength ("salt concentration") of the solution, and charge densities of the surface and the polymer. A common, counterintuitive, finding is a range of salt concentration over which the amount of adsorbed polyelectrolyte *increases* as electrostatic interactions are tempered by the addition of salt. After an adsorption maximum, higher salt concentrations then produce the expected gradual desorption of polyelectrolyte. In this work, the salt response of the adsorption of the same narrow molecular weight distribution polycation, poly(N-methyl-4-vinyl pyridinium), PM4VP, to a variety of surfaces was explored. Oxide powders for adsorption included Al_2O_3, SiO_2, Fe_2O_3, Fe_3O_4, TiO_2, ZnO and CuO. Planar surfaces included silicon wafer, mica, calcium carbonate and CaF_2 single crystals. The PM4VP was radiolabeled with ^{14}C so that sensitive, sub-monolayer amounts could be detected. The position of the peak maximum, or the lack of a peak, in response to added salt was used to rank the electrostatic component of the interaction. The importance of charge regulation, a shift in the surface pK_a in response to solution species, was highlighted as a mechanism for adsorption on the "wrong" side of the isoelectric point, and also as a factor contributing to the difficulty of reaching the totally desorbed state even at the highest salt concentrations.

INTRODUCTION

The charge carried by polyelectrolytes endows them with water solubility and also provides a mechanism for attractive interactions with opposite charges. Applications for this affinity range from stabilizing or destabilizing suspended particles or colloids to constructing ultrathin films via the layer-by-layer assembly process.[1-2] Large quantities of polyelectrolytes are used as flocculants for treating types of suspensions in water treatment,[3] in papermaking,[4] in biotechnology, and for mineral processing.[5] Particle bridging by polyelectrolytes enables their use in soil stabilization.[6-7]

Surfaces in the environment are often oxides, which means that the state of surface charge is a strong function of pH and other factors. Research on the vast number of possible surface/polyelectrolyte combinations includes a focus on the ionic strength (i.e. salt concentration) of the aqueous media in which the surface is immersed. Salt is used to weaken charge-charge interactions, whether by a site-specific mechanism, or by electrostatic screening. Unlike the adsorption of ions, polyelectrolytes often display an increase, then a decrease, in thickness/adsorbed amounts with increasing [salt].[8-13] This complex response to [salt], modeled in various theories,[12, 14-15] is an example of adsorbed amounts of polymer counterintuitively *increasing* with *weaker* interactions.[16-18]

In the presence of an adsorbing charge, the surface dissociation equilibrium is shifted towards a more ionized state, illustrated in Scheme 1 for the example of a surface hydroxyl. This process, known as charge regularization, CR, occurs in proteins,[19-20] between synthetic polyelectrolytes[21-22,23] and on mineral surfaces.[24-25]

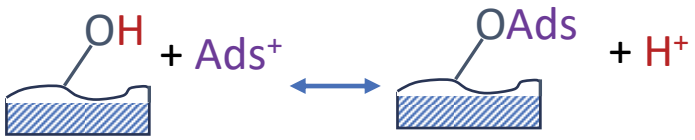

Scheme 1. In the site-binding model of charge regulation, charged species Ads^+ competes for surface charged sites, displacing H^+ and shifting the apparent pK_a of the surface.

Though the term charge regulation was introduced in the 1970s,[26] the interplay of isoelectric point and degree of polymer/protein association (for example between gelatin and gum arabic[27]) has been known for longer. A reported isoelectric point under one set of conditions may shift substantially under another set. Tsuchida and Osada[21] used the shift in pK_a of poly(methacrylic acid) on complexing with a cationic oligomer to estimate association constants as a function of polycation chain length. CR complicates predictions as to whether a polyelectrolyte will adsorb at a specific pH.

Most surfaces in most environments carry a net negative charge. Thus, polycation adsorption is widely used and studied. Polycations with pH insensitive charges usually bear quaternary ammoniums while amine pendant groups provide pH responsive repeat units.[28] Examples of the former include poly(diallyldimethylammonium), PDADMA,[13, 29-34] quaternized poly(vinylpyridines),[9-10, 12, 35-36] and quaternary ammonium acrylamides (often copolymerized with

neutral acrylamide units).[37] Examples of the latter include polyallylamine,[28, 38] polyacrylate amines,[11] and poly(ethyleneimine).[39]

Given the extensive use of polyelectrolytes in many industries, a better idea of the relative strengths of polyelectrolyte-surface interactions is needed. Motivated by our recent studies on the interaction strengths between various pairings of oppositely-charged repeat units in polyelectrolytes,[40] we wanted to rank the relative interaction strengths of oxide surfaces using the identical polycation. In a mechanism based on charge-charge interactions, sufficiently high [salt] should desorb PE molecules from the surface. The present work explores categories of polyelectrolyte adsorption on metal oxide powders in response to added ionic strength. Also included are a few planar substrates.

EXPERIMENTAL METHODS

Materials. Poly(4-vinylpyridine), (P4VP, molar mass 200 000), methanol, ethyl acetate, acetone, potassium chloride, and sodium chloride were used as received from Sigma-Aldrich. Iodomethane, dimethylformamide (DMF), molecular sieve 3A, and sodium acetate trihydrate were obtained from Fisher Scientific. Boric acid, sodium hydroxide, sodium bicarbonate, acetic acid (1.00 ± 0.005 N), and sodium carbonate (anhydrous) were used as received from VWR chemicals. Polyethylene glycol, D-sorbitol and ethylene glycol were used as received from Aldrich. Metal oxide powders Al_2O_3 acidic (99.9%), Al_2O_3 basic (99.9%), Al_2O_3 neutral (99.9% activated), rutile (98%, TiO_2), zinc oxide (96%, ZnO), silicon oxide (99.9%, SiO_2), magnetite (99%, Fe_3O_4), hematite (99.9%, Fe_2O_3) and copper oxide (99.9%, CuO) were from Sigma-Aldrich.

To prepare metal oxide powders used in this study, the “fines” or particles smaller than about 1 μm were removed by dispersing 3 g of each metal oxide powder in 50 mL H_2O and allowing the suspension to settle sequentially for 0.5, 1, 2, 4, 8, & 16 h. The cloudy supernatant was removed from the samples at each time point and the powders were redispersed in another 50 mL of water. The powders obtained were then dried under vacuum for 3 days. All dry powders except magnetite were transferred into platinum crucibles and annealed in air in a furnace for 4 h at 600 ^oC. Planar single crystal surfaces $CaCO_3$ 1-0-0 (10 x 10 x 0.5 mm) and CaF_2 1-1-1 (10 x 10 x 0.5 mm) were obtained from MTI. Muscovite mica, V-1 quality (25 x 75 mm; 0.26 – 0.31 mm thickness) was from Electron Microscopy Sciences. Silicon wafer (silicon 1-0-0, double-side-polished prime grade, 0.5 mm thick) was from Okmetic. Planar surfaces were cleaned with a Harrick plasma cleaner using air at ~150 mTorr for 30 min. Double-sided polished silicon wafers were cleaned with 3:1 H_2SO_4:H_2O_2 “piranha” solution for 30 min, rinsed in deionized water and dried under a stream of N_2.

Fractionation of P4VP. Fractions of narrow molecular weight distribution (Đ = M_w/M_n) were obtained by fractional precipitation of poly(4-vinylpyridine) from methanol with ethyl acetate. 10 g of P4VP were dissolved in 100 mL of methanol and about 225 mL of ethyl acetate was added with stirring (600 rpm) to the first sign of turbidity. The cloudy solution was centrifuged at 7000 rpm for 30 min to remove the first fraction. Four other fractions of decreasing molecular weight were collected after sequential addition of more aliquots of 1 - 2 mL of ethyl acetate to the supernatant. The recovered masses (Figure 1 Supporting Information) were recorded after drying the samples under vac for 2 days at 120 ^oC.

Quaternization of P4VP for molecular weight determination. Methylated P4VP was synthesized by treating P4VP with iodomethane (1:2 molar ratio) in oxygen-free conditions. In a 3-neck 50 mL round bottom flask, 0.5 g (4.8 mmol) of a P4VP fraction was dissolved in 10 mL of dry DMF (dried for 24 h with activated molecular sieve 3A). 1.37 g (9.6 mmol) iodomethane was added to the solution and the reaction proceeded under Ar for 24 h at room temperature. The solution went from a transparent to a yellow color as the reaction proceeded. Once the reaction was complete, quaternized P4VP, PM4VP, was transferred into a centrifuge tube and precipitated with acetone. The compound was isolated via centrifugation at 7000 rpm for 30 min and then dissolved in water and reprecipitated with acetone three times to remove impurities. This procedure was repeated for the other fractions and all samples were then freeze dried for 3 days. The resulting polymers were characterized by ^{1}H NMR spectroscopy using a Bruker Avance III 600 MHz NMR with 128 scans averaged. See Supporting Information Figures S2 and S3 for examples of NMRs.

Molecular weight determination. Molecular weight measurements were performed on fully-methylated P4VP, which was water soluble and provided well-behaved separations (see Supporting Information, Figure S4 and Table S1 Supporting Information).

Radiolabeled Methylation of P4VP. In a sealed vial, 141 mg of dry CH_3I was added to 1 mCi of $^{14}CH_3I$ (59 mCi mmol^{-1}, ViTrax Radiochemicals) in 666 µL of toluene dried with activated molecular sieve. The alkylation (Scheme 2) was carried out as follows; 52.5 mg of dry PVP (*Fraction 4*, Đ = 1.18) were dissolved in 3 mL of dry DMF in a 3-neck round bottom flask and stirred under Ar. The labeled methyl iodide solution was added to the mixture and the flask was kept under Ar at 4°C for 4 h. The solution was then allowed to react for 24 h at room temperature. The yellow precipitate was dissolved in water, reprecipitated with acetone and washed with hexane to remove impurities. The yield of the reaction was 80 % and the resulting sample was dissolved in H_2O to prepare a standard solution of 80 mM. The degree of alkylation was verified to be > 98 % using FTIR spectroscopy performed on Si wafers. In this experiment, drops of P4VP and radiolabeled PM4VP were air-dried on double-side-polished Si wafers and the FTIR spectra were acquired at a resolution of 4 cm^{-1} averaging 100 scans using a Thermo Nicolet Avatar 360 spectrometer. A bare Si wafer was used as a background and the measurements were done at room temperature (23 ± 2 °C).

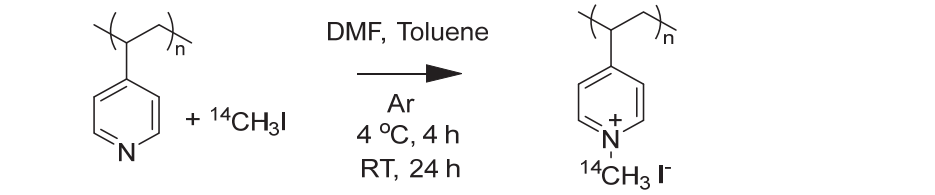

Poly(4-vinylpyridine) Poly(N-methyl-4-vinyl pyridinium iodide)

Scheme 2. Procedure for radiolabeled methylation of P4VP.

SEM Imaging. Samples of metal oxide powders were prepared by putting a drop of metal oxide suspension (100 mg powder in 5 mL water) on a carbon conductive tape and dried overnight in a

desiccator. The SEM images (see Supporting Information Figure S5) were acquired using a FEI NovaSEM 400 after coating the samples with a 4-nm layer of iridium using a Cressington HR 208 sputter coater. The acceleration voltage was set to 15 kV and a working distance of 5 mm was employed with an Everhart-Thornley detector.

Surface Area. The surface area of powders was measured via BET isotherms (see Supporting Information Table S2). Ideally, surface areas would provide the absolute amount of polymer coverage, for example in mg m^{-2}. Unfortunately, it is not known what fraction of this area is accessible to polymer and the SEM images of the particles in Supporting Information S5 clearly show aggregates of smaller particles. However, the main objective of this work was to compare the interaction strength between surface and polymer by challenging this interaction with increasing salt concentration. Two pH values were selected, 4.5 and 9.5, set by the appropriate buffer solutions.

Radiolabeled Polymer Adsorption. The relative amount of polyelectrolyte adsorbed to oxides at various [KBr] was determined by proximity radio-counting. The procedure is illustrated in Figure 1. A piece of clean plastic scintillator (SCSN 81, 3 mm thick, Kuraray Inc.) was glued with epoxy resin to the end of a 1-inch diameter glass tube. The resulting cell was placed on the end of a 2" diameter end-on photomultiplier tube (RCA 8850 biased at -2100 volts). Counts were acquired on a Philips PM6654C counter. The β-particles from ^{14}C-labeled polymer are only able to travel about 30 μm in the solution. Thus, only β-particles from PM4VP adsorbed to the settled powder will reach the scintillator, and also from a small amount of PE in the layer of solution adjoining the scintillator (this background contributed about 13 counts per second, cps).

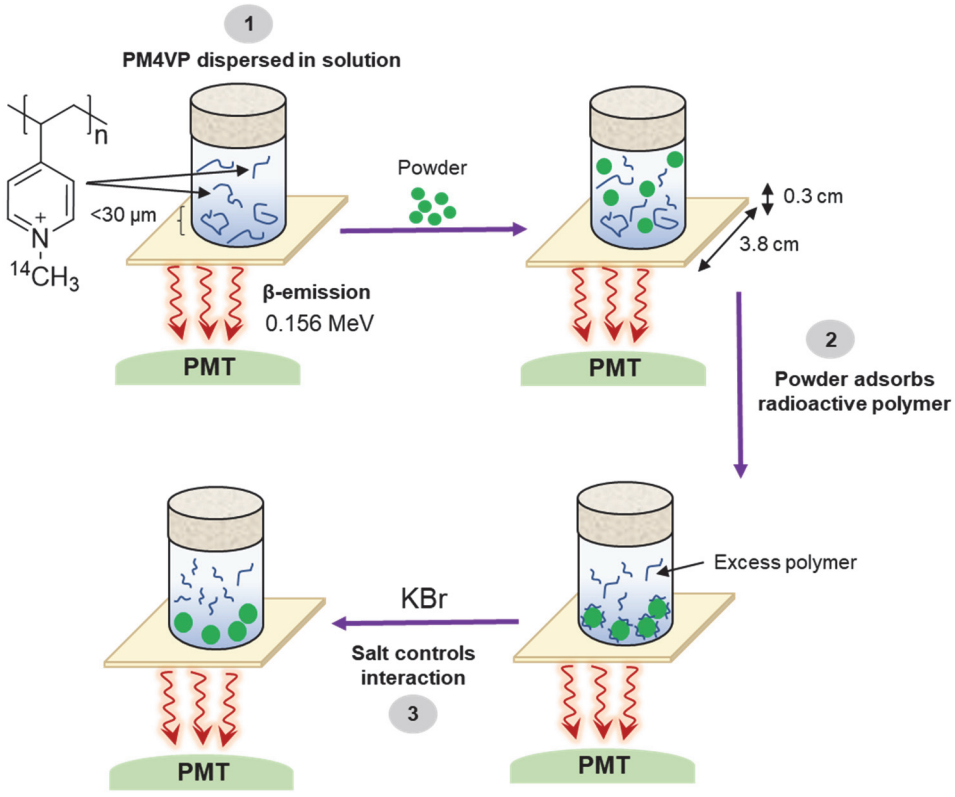

Figure 1. The proximity assay method. **1**) radiolabeled PM4VP is dissolved in a buffered solution in a scintillator-bottom reactor. ^{14}C β-emissions within a range of ~30 μm of the scintillator are detectable. **2**) Metal oxide and salt are added (with counts in between) and shaken, then allowed to settle. Radionuclides enter the β- range as metal oxides with adsorbed radioactive PM4VP settles. **3**) Subsequent salt addition modifies polymer adsorption and counts change accordingly.

In a typical radio-counting experiment, 5 mL buffer (10 mM ionic strength carbonate buffer pH 9.5, or 10 mM acetate buffer pH 4.5) and 50 μL "hot" PM4VP (80 mM, 1 Ci mol^{-1} for a concentration of 0.8 mM ^{14}C-PM4VP in the reactor) were mixed in a scintillator reactor (Figure 1) and background counts were recorded after 15 min. 100 mg of an oxide powder was added and the solution was mixed. The powder was allowed to settle completely (15-45 min, indicated by a stable count rate and a clear supernatant), and the counts were recorded again. Aliquots of 2.5 M KBr were added to the suspension to control the ionic strength of the solution. Before every measurement, the solution was shaken thoroughly and allowed to settle. All measurements were done at room temperature and the background counts were subtracted from the counts of the samples.

As a check to ensure that the powders never adsorbed all of the PM4VP in the reactor, and thus the adsorbed amount was not limited by the solution amount, 100 μL aliquots of the radioactive supernatant from each metal oxide solution were taken before the addition of any KBr to the metal oxide solution and after the final addition of salt. Each aliquot was added to 5 mL of Ecolite liquid scintillation cocktail in a 13 x 100 mm borosilicate glass tube. The counts for the resulting mixtures were recorded in triplicate for one min on a Charm II liquid scintillation counter (typical counting efficiency for ^{14}C = 68%, background < 1 count min^{-1}). At most, half of the of the available polymer was adsorbed by powders.

RESULTS AND DISCUSSION

The amount of polyelectrolyte adsorbed to a surface shows a weak dependence on molecular weight.[9, 41-42] Also, large polymers are known to displace smaller ones when they compete for adsorption sites.[35, 38] Thus, the comparison of adsorbed amounts is ideally performed with narrow molecular weight distribution, Đ, polymer. Relatively narrow Đ P4VP was prepared by fractionating a wide Đ commercial sample. Samples from the five fractions (Supporting Information Figure S1) were alkylated with methyl iodide. ^1H NMR spectra showed full alkylation (Supporting Information Figure S3) of the starting P4VP (Supporting information Figure S2). ^1H NMR spectra of all fractions also showed complete alkylation and no structural differences (Supporting Information Figure S1). Aqueous SEC-MALS was then performed on all the fractions to determine molecular weight and polydispersity (Supporting Information Figure S4). Fraction 4 (M_w = 227,000; M_n = 192,000; Đ =1.18 when methylated) was selected for radiolabeling.

Radiolabeling was done to a specific activity of about 1 Ci mol^{-1} of PM4VP repeat units using $^{14}CH_3I$. Because the isotope was supplied in toluene, which is not a good solvent for this type of alkylation (the Menshutkin reaction), the level of alkylation on the labeled PM4VP was checked using FTIR. Figure 2 shows complete disappearance of the 1414 cm^{-1} band in the starting material and a total shift of the band at ca. 1600 to ca 1650 cm^{-1}, which is evidence for complete alkylation.

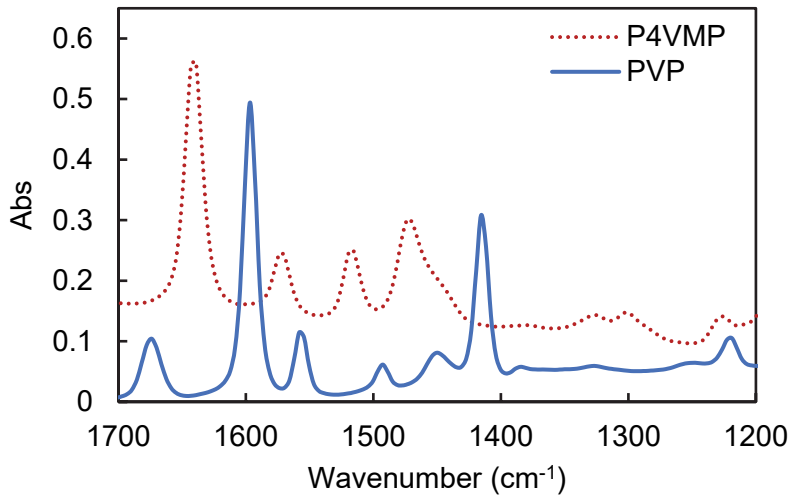

Figure 2. FTIR spectra of P4VP and radiolabeled PM4VP between 1200 and 1700 cm^{-1}. The C=C stretching band at 1600 cm^{-1} in the pyridine ring completely disappears and a new peak corresponding to the monosubstituted C=C appears at 1640 cm^{-1}. [10,43] The complete lack of bands at 1414 cm^{-1} and 1600 cm^{-1} corresponding to the unalkylated pyridine is taken as full (> 98%) methylation.[44]

KBr was chosen as the salt, rather than NaCl, because of our experience with charge-charge interactions in polyelectrolyte complexes.[45] Complexation was found to be athermal and KBr was more effective than NaCl at breaking pairs of charges between polyelectrolytes.[45] Our assumption that KBr interacts more strongly with -Surf-O-Pol^+ appears to be justified from comparison with the results of Sukhishvili and Granick, who also evaluated PM4VP adsorption on oxidized silicon, but with NaCl as salt.[10] The adsorbed amount showed a maximum at about 1 M NaCl instead of < 0.4 M KBr seen below.

The Counterion Release Mechanism. Scheme 3 illustrates the important contribution of counterion release from both PE and surface to driving adsorption. This entropic driving force has been demonstrated in polyelectrolyte complex formation[46] and protein adsorption on polyelectrolytes.[47] The Scheme makes the reasonable assumption that counterions are either "condensed" onto the polyelectrolyte backbone or surface, or they are in close proximity. Once the first repeat unit, Pol^+, of the polymer molecule attaches to the surface ("first contact"), it loses what little translational entropy it had. At low [KBr] each contact made with the surface, -Surf-O^- Pol^+, releases one KBr. There is some loss of polymer configurational entropy,[48] but this is far outweighed by the gain in counterion translational entropy. Due to multiple interaction points, polymers are high-affinity adsorbers, which means they reach their highest (plateau) coverage at exceedingly low concentrations.[41] They are difficult to desorb: a polymer chain with n repeat units, $(Pol)_n$ is still adsorbed even if n-1 repeat units are desorbed and only 1 unit is left clinging to the surface.

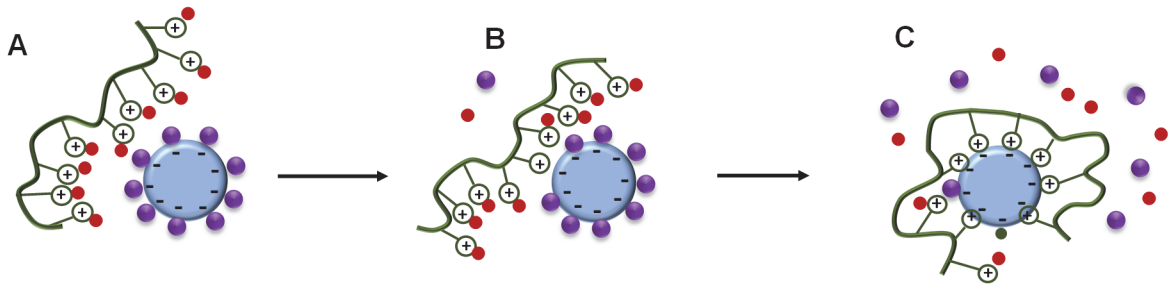

Scheme 3. Progress of counterion release. **A**; polyelectrolyte added to solution. **B**; the "first contact" is made, displacing one countercation and one counteranion. Polymer loses translational entropy. **C**; additional $Surf^{-}Pol^{+}$ pairs are made, releasing more counterions. Polymer loses configurational entropy.

Charge Regulation, Adsorption and Desorption. Ionization reactions at an amphoteric surface (capable of accepting or yielding protons) are represented in a simple site binding model by Equations 1 & 2: [32]

$$Surf-OH + K^{+}_{aq} \leftrightarrow Surf-O^{-}K^{+} + H^{+}_{aq} \quad [1]$$

$$Surf-OH + H^{+}_{aq} + Br^{-}_{aq} \leftrightarrow Surf-OH^{+}_{2}Br^{-} \quad [2]$$

The surface charges are shown with condensed counterions, forming the Stern layer, in order to emphasize CR: positive salt ions induce greater -OH ionization (pK_a shifts to lower values) in Equilibrium 1. Dissociation of some of these condensed ions leads to the diffuse layer in the Gouy-Chapman model. The competition between K^+ and H^+ shown in Equation 1 favors the H^+ by some 40 kJ under standard conditions (i.e. ΔG^o is about +40 kJ)[49] but under the experimental conditions used here $[K^+] >> [H^+]$. Additional CR is caused by PE adsorption.

$$Surf-OH + Pol^{+}Br^{-}_{aq} \leftrightarrow Surf-O^{-}Pol^{+} + H^{+}_{aq} + Br^{-}_{aq} \quad [3]$$

Thus, ions and polymers of the same charge both induce CR in the same direction, favoring adsorption at a pH where the IEP measured at low [salt] in the absence of PE suggests electrostatic interactions should be repulsive (also known as the "wrong side" of the IEP[50]). Čakara et al. demonstrate an IEP shift from about pH 3 to about 8 on Si wafer induced by the adsorption of the polycation poly(diallyldimethylammonium).[29]

Equation 4 describes competition between salt and polyelectrolyte charged units for surface sites at low [salt]. Because of the multivalent interactions offered by PE (large "n") it dominates the competition at all practical concentrations of added PE rapidly giving monolayer coverage at the lowest concentrations.

$$n(Surf-O^{-}K^{+}) + \left(Pol^{+}Br^{-}_{aq}\right)_{n} \rightarrow n(Surf-O^{-}Pol^{+}) + nK^{+}_{aq} + nBr^{-}_{aq} \quad [4]$$

Viewing salt as a competitor for surface sites, increasing [salt] displaces small molecules completely. In contrast, the macromolecular nature of a PE allows it to adopt a more coiled conformation while still maintaining surface attachments. In classical terminology, polymer not in contact with the surface exists in "loops" and "tails."[41] The weakening of polymer-surface

interactions by added salt allows more polymer to adsorb. If the response of the conformation of polyelectrolyte to [salt] is treated via electrostatics, the overall adsorbed amount can be modeled, for example by self consistent field (SCF) theory[14, 51-52] or correlation-corrected density functional theory (DFT).[12] Equation 5 represents all adsorbed Pol^+ not in contact with the surfaces as "loops."

$$n(Surf - O^- Pol^+) + m\left(Pol^+ Br^-_{aq}\right)_n \rightarrow n(Surf - O^- Pol^+)(Pol^+ Br^-)_{m,loop} \qquad [5]$$

where m,loop is the ratio of monomer units in loops to those in trains. In theory, if enough salt is added, all PE-surface interactions are broken and the entire PE molecule desorbs (Equation 6).

$$n(Surf - O^- Pol^+)(Pol^+ Br^-)_{m,loop} + nKBr_{aq} \rightarrow nSurf - O^- K^+ + (1+m)(Pol^+ Br^-_{aq})_n \qquad [6]$$

SCF & DFT do a good job at predicting a maximum in adsorbed PE versus [salt], but a nonelectrostatic interaction term must be added to account for the near-universal observation that some PE remains adsorbed even at the highest [NaCl].[12, 14, 51] Nonelectrostatic interactions (dipolar, hydrophobic,[53] H-bonding, van der Waals etc.) are widely invoked to explain the lack of complete desorption at high [salt][12, 51, 54] and the adsorption of charged polymers on nominally neutral or like-charge surfaces.[34, 55] Other potential driving forces are not directly revealed in this set of Equations. For example, specific interactions due to the chemical nature of adsorbing charges provide additional enthalpic terms for a preference of charge type at the interface. If there are changes in protonation state, the enthalpy of ionization, not usually explicitly included, also moderates adsorption. For example, the ionization enthalpy of carboxylates is low (for example, about zero kJ mol^{-1} for acetic acid at 25 °C[56]) but is much more substantial for amines.[57] In addition, the solvent quality for PEs in water decreases with high [salt], which also induces the chain to linger on the surface. An attempt was made to displace PM4VP from the Si wafer in 1.2 M KBr by adding 100 µL of a 10 wt% solution of poly(ethylene glycol), PEG, molecular weight 8000, as a non-electrostatic competitor. Adsorbed amounts decreased little (Supporting Information Figure S7). 100 mL of 80 mM sorbitol was also added at the same salt concentration, and the adsorbed amount decreased by only 17% (data not shown).

Classes of Salt Response

The selection of nine oxide powders was intended to represent substrates commonly used to evaluate PE adsorption. Adsorption to a steady-state coverage occurs rapidly.[33, 39] If adsorption were controlled by charge-charge interactions only, one might expect the amount of PE at the solid/liquid interface to approach zero at sufficiently high salt concentration (see Equation 6). Though coverage generally decreased at the highest [KBr], it never dropped to zero. Instead, the salt response is classified according to whether a maximum was observed. In the "pre-peak" systems, a low coverage at low [KBr] evolves to a maximum, then falls off with higher [salt]. These may also be considered "well behaved" in the sense that they are explained by theory.[12, 14, 51] "Post-peak" systems simply start with a high surface PE, which drops as more salt is added. "Nonadsorbing" examples do not show coverage at any [salt].

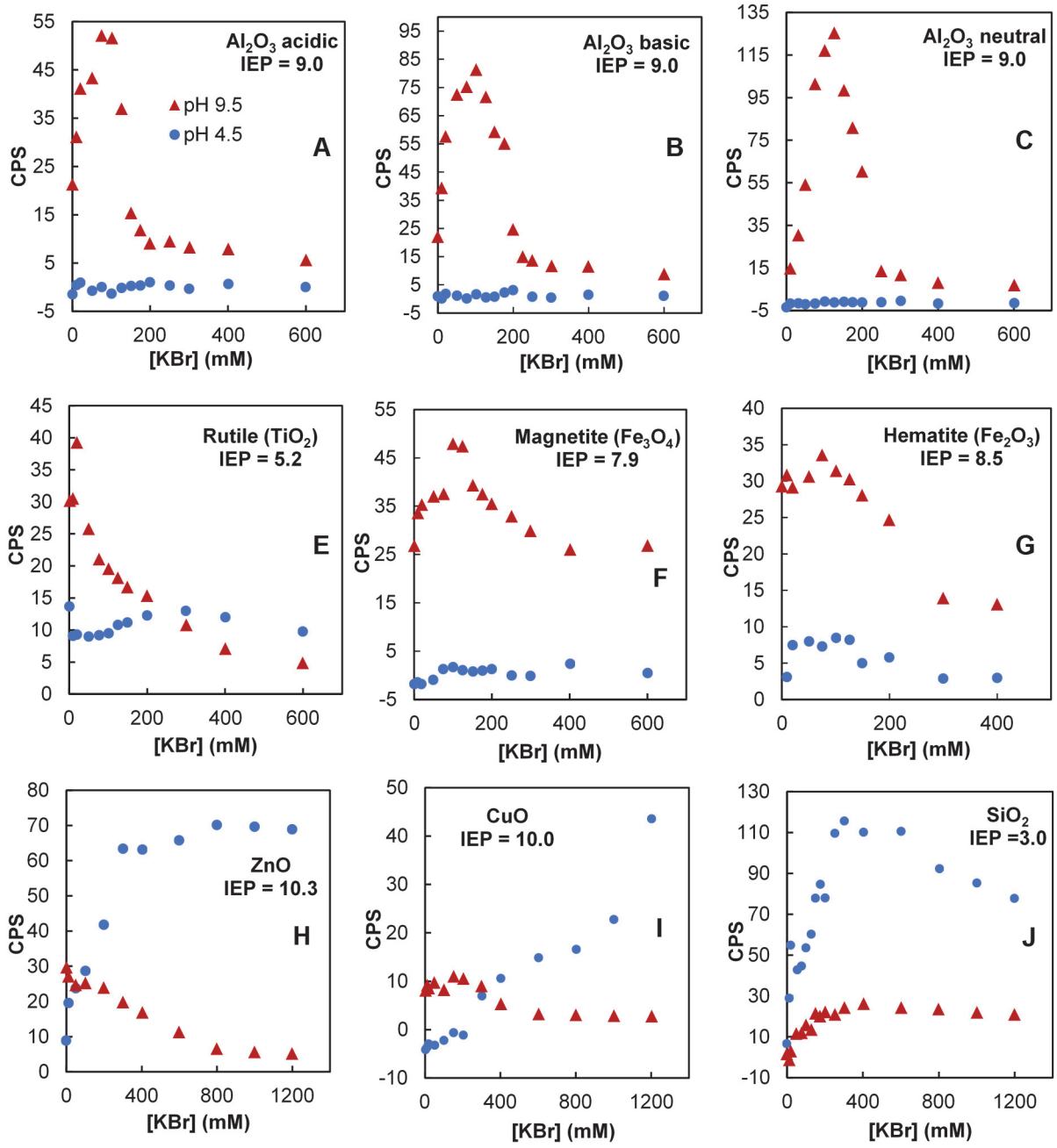

Figure 3. A-J. Relative amounts of absorbed PM4VP (*Fraction 4*, M_w = 227,000, M_n = 192,000) in counts per second, *versus* [KBr] for oxide powders. Buffered at pH = 9.5 (▲) and pH = 4.5 (●). Room temperature. Nominal isoelectric point, IEP, is given. Background has been subtracted from all CPS shown. Precision is ± 2 cps.

Accordingly, the three aluminas at pH 9.5 in Figure 3 exhibit the best-defined maximum, then fall to low (relative) absorbed amounts. With an IEP at 9.0 the complete lack of adsorption at pH 4.5, where the surface should be strongly positive, is also expected. Rutile, magnetite and hematite exhibit a smaller maximum at a pH above their IEP (Figure 3) with little to no adsorption at low pH. A low adsorption maximum for rutile and hematite at pH 4.5 might be a result of regulation to

a lower IEP by added polymer. In other words, the surface is forced to remain negative by absorbing PE. In polyelectrolytes, proteins, and peptides charge regulation can shift a pK_a by more than three units.[20, 23, 58]

ZnO and CuO are both post-peak absorbers at high pH, and the absorbed amount almost reaches zero at high [salt]. The [KBr] was taken to higher values, 1.2 M, for these two oxides to make sure the absorbed amount had reached a plateau close to zero (Figure 3). The absorbed amounts for ZnO and CuO increased with [KBr] at pH 4.5 (Figure 3). These two oxides are likely dissolving at this pH[59] and could be forming a gel-like structure with higher polycation sorption capacity. It is also possible that nonelectrostatic forces, such as π-cation interactions between the pyridine and metal ions, may be assisting adsorption.

Silica is an outlier in some respects. Untreated silica surfaces in monovalent salt rarely turn positive, even at low pH. Unlike amphoteric surfaces, the IEP is taken as the point where surfaces eventually reach zero charge, rather the point the charge switches in sign. Figure 3 shows an increase in adsorbed amount versus [KBr] at both pH 4.5 and 9.5. The peak is more prominent for the more weakly-charged surface and falls little with additional KBr.

Planar surfaces. PM4VP adsorption on a series of planar surfaces is shown in Figure 4. The main substrate of interest is Si wafer. $CaCO_3$, CaF_2 and mica were added as other representatives of planar inorganic surfaces. Because the surface areas were known for these samples, absolute coverage, in mg m^{-2}, could be measured. The confidence level in the accuracy of the measurement is high because of the simplicity of the radioisotope labeling technique. Both accuracy and precision are estimated to be +/- 10%.

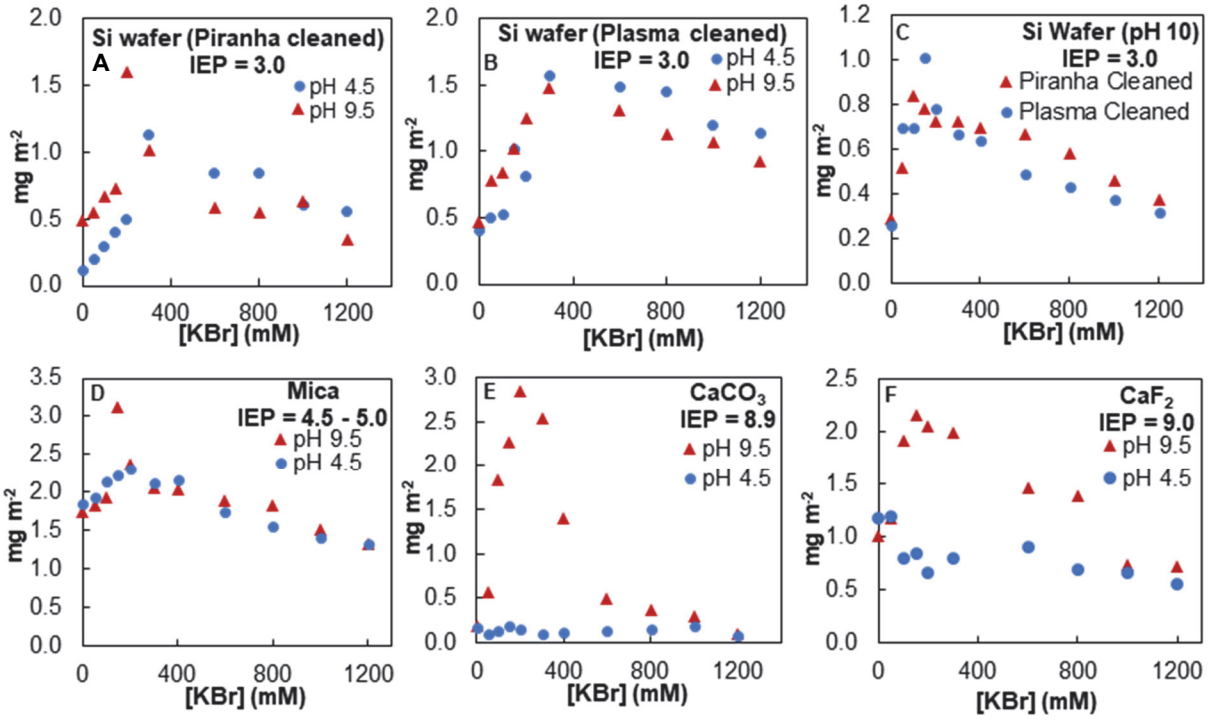

Figure 4. Adsorbed amount of PM4VP (*Fraction 4*, M_w = 227,000, M_n = 192,000) as a function of [KBr] for smooth (single crystal) planar surfaces. Room temperature. Precision is ± 0.2 mg m^{-2}. Calibration curves are given in Supporting Information Figure S8.

Figures 4 A-C focus on adsorption at smooth silicon wafers, which all carried a native oxide layer of thickness about 2 nm. The method of surface cleaning differed between Figures 4A and 4B: piranha versus plasma. Figure 4C increases the pH slightly from 9.5 to 10.0. All measurements of PM4VP on Si wafer as a function of [salt] agree reasonably well with prior literature using NaCl.[9-10, 12] The adsorption peaks were quite sharp and occurred in the range 0.15 - 0.3 M KBr for all pH. The lowest coverage (Figure 4A-C) occurred at minimal [KBr]. Desorption was incomplete up to 1.2 M KBr, and even up to 2.2 M KBr (data not shown). While the adsorption behavior on plasma- *versus* piranha-cleaned surfaces showed little difference at high pH (Figure 4C), slightly more polymer adsorbed on the plasma-cleaned Si than on piranha-cleaned Si at lower pH (compare Figures 4A and 4B). DeRosa et al.[60] found piranha treatment yielded more surface silanols on silica than did plasma exposure. A surface with more silanols would interact more strongly with PM4VP and produce lower adsorbed amounts according to the logic used here.

Mica showed adsorption profiles at pH 4.5 and 9.5 similar to those on Si (Figure 4D). Profiles of PM4VP on mica (about 34 μC cm^{-2}) are similar to those of a quaternary ammonium acrylamide[37] and similar to Si wafer. Minerals such as mica[37] and clay[61] are known to exchange their surface ions. In some cases (Si wafer, mica), the maximum adsorbed amount was curiously sharp. This feature has not been reported previously, probably because the [KBr] increments were small enough here to capture this jump.

Adsorption on $CaCO_3$ (Figure 4E) at pH 9.5 showed a strong peak and complete desorption at the highest [KBr]. No adsorption was observed at pH 4.5, where the $CaCO_3$ is probably dissolving. Because calcite ($CaCO_3$) is not an oxide, the IEP is not a direct function of pH. Instead, Ca^{2+} and CO_3^{2-} ions determine the potential, and pH acts indirectly via dissolved CO_2 (e.g. Surf-CaOH + CO_2 = $CaCO_3^-$ + H^+).[62] In fact, $CaCO_3$ is slightly water-soluble and surface ions are in dynamic equilibrium with solution ions.[62] Unlike SiO_2, direct ion exchange of PE segments with the surface is possible, e.g.

$$Surf - Ca + 2Pol_{aq}^{+} \rightarrow Surf - Pol_2^{+} + Ca_{aq}^{2+}$$

Note the height of the adsorption peak and the fact that PM4VP is eventually completely displaced by KBr (Figure 4).

Ranking Interactions. The initial goal of ranking the PE-surface interaction energies by the response to [salt] was confounded by the complexity of PE adsorption in general. In particular, adsorbed PE could rarely be completely displaced by sufficient KBr. An overall dependence of adsorption on pH demonstrated the role of surface charge. A quantitative ranking has not been reported directly in the literature. A summary of PE adsorption in response to increasing [NaCl] is given in Figure 5.

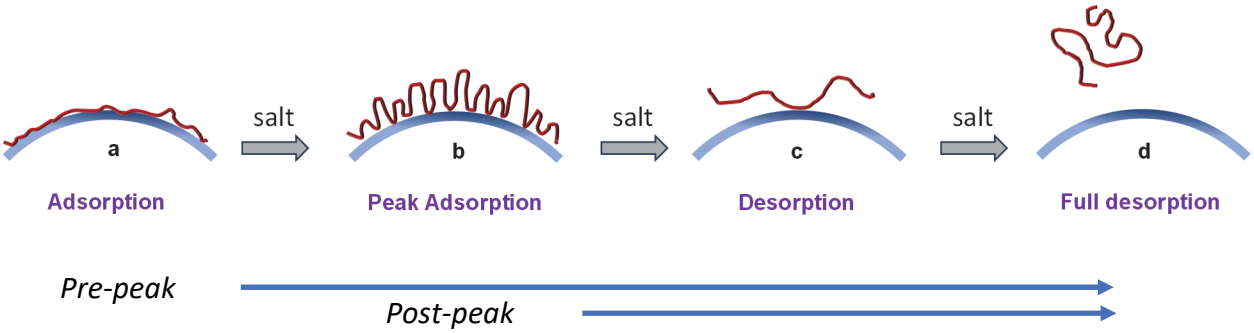

Figure 5. Representation of surface coverage *versus* [NaCl] for polyelectrolyte adsorption. Pre-peak systems exhibit the entire response, whereas post-peak only decrease with increasing [KBr].

Using computer simulations, Portnov and Potemkin recently predicted[63] that a higher [salt] would be needed to desorb a polyelectrolyte from a charged surface than would be required to separate the same molecule from a polymer with the same charge as the surface. Unfortunately, surfaces and polyelectrolytes usually have strongly different chemical compositions. For example, PM4VP is easily separated from fully-charged poly(methacrylic acid) in > 0.58 M NaCl,[64] yet does not release from silica, as shown here and elsewhere. Does this mean silica offers more non-electrostatic interactions, or does -Si-O^- interact more strongly with the M4VP charge? We are not able to answer this question. However, charge regulation means that the more salt is added, the more surface charge is revealed (Equation 1), which interacts more strongly with PM4VP.

The pH range over which silanols become ionized is extremely broad. For comparison, a small molecule following the Henderson-Hasselbalch equation spans 1 % to 99% ionization within ± 2 pH units on either side of its pK_a. About 1% of silanols of concentration of 7.6 x 10^{-6} mol m^{-2} (73 µC m^{-2})[65] on SiO_2 are ionized at pH 3 and only 22% of them are ionized at pH 10,[66] severe hydrolysis of the silica setting in at pH 11.[67] As with polyacids such as poly(acrylic acid), ionization is increasingly disfavored as the charge density increases during ionization.[68] CR occurs because either K^+ or Pol^+ neutralizes charge, allowing more ionization at a particular pH (i.e. shifting the apparent pK_a lower).[23] This increased surface charge density can be expected to extend the range of [salt] over which polyelectrolyte remains on the surface. Hoogeveen et al. remarked on a lack of reversibility of PM2VP on SiO_2 compared to TiO_2 implying stronger adsorption in the former.[35]

A rough ranking of PM4VP/surface interaction strength at pH 9.5 may be assembled from the data in Figures 3 and 4. The post-peak surfaces were assumed to be the weakest and the rest are ordered according to the KBr concentration at the adsorption maximum. With an error of +- 0.03 M the differences between many surfaces are not enough for comprehensive ranking, but SiO_2 and $CaCO_3$ are clearly at the top and rutile is clearly towards the bottom (see Table 1). The ranking in Table 1 is done on a “whole chain” basis rather than a per segment basis, meaning that there is no information on the differences between surfaces, if any, of the fraction of segments adsorbed as loops versus trains under the same conditions.

Table 1. Approximate ranking of interaction strengths, from high to low, between PM4VP and surfaces using the [KBr] for peak adsorption.

Rank	Mineral	$[KBr]_{peak}$
1	SiO_2	0.32
2	$CaCO_3$	0.19
3	Mica	0.15
4	CaF_2	0.15
5	Magnetite	0.11
6	Al_2O_3	0.094
7	Hematite	0.071
8	Rutile	0.017
9	CuO	[a]n/a
10	ZnO	[a]n/a

[a]post-peak

+/- 0.03 M

pH = 9.5, room temperature

There are reports of a few cases where polyelectrolytes desorb with sufficient [salt]. It appears that a low surface or polyelectrolyte charge density helps in this respect. Hansupalak and Santore[11] reported full desorption of a polyaminoacrylate, poly(methylamino ethyl methacrylate, PDMAEMA), from silica at about 0.1 M NaCl under pH conditions (pH > 9.3) that were sufficiently high to remove most of the charge from the weak polyelectrolyte (although silica is highly charged under these conditions). The authors used this finding to explore desorption and exchange rates under various conditions,[69] and found desorption and exchange (of labeled for unlabeled PDMAEMA) were only possible close to the "desorption edge." If a highly-charged polyelectrolyte has sufficiently low molecular weight, desorption may be observed,[31] and desorption has also been reported for pH-insensitive polyelectrolytes with low charge density (i.e where charged units are heavily diluted with uncharged units).[37]

Conclusions

This work was directed towards evaluating the relative affinity of the same fully-charged polyelectrolyte for different oxide surfaces by using KBr to challenge surface-PE electrostatic interactions. At high [KBr] and pH, PM4VP could be nearly fully desorbed from only a couple of substrates: alumina and calcium carbonate. For most of the surfaces a maximum of absorbed amount versus [KBr] was observed, in accord with the known response of many polyelectrolytes.[11, 14, 70, 35, 71] Three categories of adsorption strength were developed. First, systems which exhibited a well-defined peak in adsorbed amount as a function of [salt], termed "prepeak," were strong enough to show low adsorption at [salt] → 0, followed by high adsorption as desorbed segments were still indirectly anchored to the surface. Prepeak responses were ranked according to the [KBr] at the peak. Second was "postpeak," where adsorbed amounts decreased with the addition of any KBr. A low pH was effective at preventing adsorption in amphoteric surfaces, probably because they were positive and actively repelled the PM4VP. The silicon oxide surface on Si wafer strongly interacted with PM4VP at high and low pH, possibly aided considerably by surface charge regulation. Because CR exposes a higher surface charge density (Equations 1 and 3) it counteracts the desorption effects of added salt (Equation 6)

promoting adsorption to a higher [salt]. Complete polyelectrolyte desorption is effected by a combination of low surface or polymer charge and high [salt].

Author Information

Corresponding Author

Joseph B. Schlenoff – *Department of Chemistry and Biochemistry, The Florida State University, Tallahassee, Florida 32308-4390, United States;* orcid.org/0000-0001-5588-1253; Email: jschlenoff@fsu.edu

Authors

John Akintola- *Department of Chemistry and Biochemistry, The Florida State University, Tallahassee, Florida 32308-4390, United States*.

Samir Abou Shaheen- *Department of Chemistry and Biochemistry, The Florida State University, Tallahassee, Florida 32308-4390, United States*; orcid.org/0000-0003-3258-5341

Qiang Wu *Department of Industrial and Manufacturing Engineering, FAMU-FSU College of Engineering, Tallahassee, Florida, 32310-6046, United States*

Notes

The authors declare no competing financial interest.

Acknowledgments

This work was supported by grants DMR-1809304 and DMR-2103703 from the National Science Foundation.

Supporting Information

^{1}H NMR spectra of P4VP and methylated P4VP; details for SEC-MALLS procedure; SEC chromatograms of methylated P4VP; SEM images of the oxide powders used; example BET isotherm; summary of metal oxide properties and isoelectric points; attempt at breaking non-electrostatic interactions; calibration plots for radiolabeled PM4VP on planar surfaces. This information is available free of charge.

REFERENCES

1. Decher, G.; Schlenoff, J. B. *Multilayer Thin Films: Sequential Assembly of Nanocomposite Materials, 2nd Ed.*; Wiley-VCH: Weinheim, 2012.

2. Ariga, K.; Lvov, Y.; Decher, G. There Is Still Plenty of Room for Layer-by-Layer Assembly for Constructing Nanoarchitectonics-Based Materials and Devices. *Physical Chemistry Chemical Physics* **2022,** *24*, 4097-4115.
3. Bolto, B.; Gregory, J. Organic Polyelectrolytes in Water Treatment. *Water Res* **2007,** *41*, 2301-24.
4. Khan, N.; Renfroe, A. R.; von Grey, P.; Witherow, H. A.; Brettmann, B. K. The Influence of Electrostatic Interactions in Polyelectrolyte Complexes on Water Retention Values of Cellulose Nanofiber Slurries. *Cellulose* **2022,** *29*, 9163-9181.
5. Ma, J.; Fu, K.; Jiang, L.; Ding, L.; Guan, Q.; Zhang, S.; Zhang, H.; Shi, J.; Fu, X. Flocculation Performance of Cationic Polyacrylamide with High Cationic Degree in Humic Acid Synthetic Water Treatment and Effect of Kaolin Particles. *Separation and Purification Technology* **2017,** *181*, 201-212.
6. Yamaguchi, A.; Kanashiki, N.; Ishizaki, H.; Kobayashi, M.; Osawa, K. Relationship between Soil Erodibility by Concentrated Flow and Shear Strength of a Haplic Acrisol with a Cationic Polyelectrolyte. *CATENA* **2022,** *217*, 106506.
7. Huang, J.; Makhatova, A.; Kogbara, R.; Masad, E.; Sukhishvili, S.; Little, D. Mechanical Properties of Palygorskite Clay Stabilized with Polyelectrolytes. *Transportation Geotechnics* **2023,** *43*, 101124.
8. Shubin, V. Adsorption of Cationic Polyacrylamide onto Monodisperse Colloidal Silica from Aqueous Electrolyte Solutions. *Journal of Colloid and Interface Science* **1997,** *191*, 372-377.
9. Hoogeveen, N. G.; Cohen Stuart, M. A.; Fleer, G. J. Polyelectrolyte Adsorption on Oxides: I. Kinetics and Adsorbed Amounts. *Journal of Colloid and Interface Science* **1996,** *182*, 133-145.
10. Sukhishvili, S. A.; Granick, S. Polyelectrolyte Adsorption onto an Initially-Bare Solid Surface of Opposite Electrical Charge. *The Journal of Chemical Physics* **1998,** *109*, 6861-6868.
11. Hansupalak, N.; Santore, M. M. Sharp Polyelectrolyte Adsorption Cutoff Induced by a Monovalent Salt. *Langmuir* **2003,** *19*, 7423-7426.
12. Xie, F.; Nylander, T.; Piculell, L.; Utsel, S.; Wågberg, L.; Akesson, T.; Forsman, J. Polyelectrolyte Adsorption on Solid Surfaces: Theoretical Predictions and Experimental Measurements. *Langmuir* **2013,** *29*, 12421-12431.
13. Geonzon, L. C.; Kobayashi, M.; Sugimoto, T.; Adachi, Y. Adsorption Kinetics of Polyacrylamide-Based Polyelectrolyte onto a Single Silica Particle Studied Using Microfluidics and Optical Tweezers. *Journal of Colloid and Interface Science* **2023,** *630*, 846-854.
14. Van de Steeg, H. G. M.; Cohen Stuart, M. A.; de Keizer, A.; Bijsterbosch, B. H. Polyelectrolyte Adsorption : A Subtle Balance of Forces. *Langmuir* **1992,** *8*, 2538-2546.
15. Chang, Q.; Jiang, J. Sequence Effects on the Salt-Enhancement Behavior of Polyelectrolytes Adsorption. *Macromolecules* **2022,** *55*, 897-905.
16. Ernstsson, M.; Dedinaite, A.; Rojas, O. J.; Claesson, P. M. Two Different Approaches to XPS Quantitative Analysis of Polyelectrolyte Adsorption Layers. *Surface and Interface Analysis* **2022,** *55*, 26-40.
17. Schlenoff, J. B.; Dharia, J. R.; Xu, H.; Wen, L.; Li, M. Adsorption of Thiol-Containing Copolymers onto Gold. *Macromolecules* **1995,** *28*, 4290-4295.
18. Moore, D.; Arcila, J. A.; Saraf, R. F. Electrochemical Deposition of Polyelectrolytes Is Maximum at the Potential of Zero Charge. *Langmuir* **2020,** *36*, 1864-1870.
19. Harris, T. K.; Turner, G. J. Structural Basis of Perturbed Pka Values of Catalytic Groups in Enzyme Active Sites. *IUBMB Life* **2002,** *53*, 85-98.

20. Isom, D. G.; Castañeda, C. A.; Cannon, B. R.; García-Moreno E, B. Large Shifts in pKa Values of Lysine Residues Buried inside a Protein. *Proceedings of the National Academy of Sciences* **2011,** *108*, 5260-5265.
21. Tsuchida, E.; Osada, Y. The Rôle of the Chain Length in the Stability of Polyion Complexes. *Die Makromolekulare Chemie* **1974,** *175*, 593-601.
22. Zheng, B.; Avni, Y.; Andelman, D.; Podgornik, R. Charge Regulation of Polyelectrolyte Gels: Swelling Transition. *Macromolecules* **2023,** *56*, 5217-5224.
23. Digby, Z. A.; Yang, M.; Lteif, S.; Schlenoff, J. B. Salt Resistance as a Measure of the Strength of Polyelectrolyte Complexation. *Macromolecules* **2022,** *55*, 978-988.
24. Yates, D. E.; Levine, S.; Healy, T. W. Site-Binding Model of the Electrical Double Layer at the Oxide/Water Interface. *Journal of the Chemical Society, Faraday Transactions 1* **1974,** *70*, 1807-1818.
25. Wolterink, J. K.; Koopal, L. K.; Stuart, M. A. C.; Van Riemsdijk, W. H. Surface Charge Regulation Upon Polyelectrolyte Adsorption, Hematite, Polystyrene Sulfonate, Surface Charge Regulation: Theoretical Calculations and Hematite-Poly(Styrene Sulfonate) System. *Colloids and Surfaces A* **2006,** *291*, 13-23.
26. Ninham, B. W.; Parsegian, V. A. Electrostatic Potential between Surfaces Bearing Ionizable Groups in Ionic Equilibrium with Physiologic Saline Solution. *Journal of Theoretical Biology* **1971,** *31*, 405-428.
27. Bungenberg de Jong, H.; Dekker, W. Zur Kenntnis Der Lyophilen Kolloide: XXV. Mitteilung. Über Koazervation Ii: Komplexkoazervation Des Systems Gummiarabikum-Gelatine. *Kolloid-Beihefte* **1935,** *43*, 143-212.
28. Szilagyi, I.; Trefalt, G.; Tiraferri, A.; Maroni, P.; Borkovec, M. Polyelectrolyte Adsorption, Interparticle Forces, and Colloidal Aggregation. *Soft Matter* **2014,** *10*, 2479-2502.
29. Čakara, D.; Kobayashi, M.; Skarba, M.; Borkovec, M. Protonation of Silica Particles in the Presence of a Strong Cationic Polyelectrolyte. *Colloids Surfaces A* **2009,** *339*, 20-25.
30. Holkar, A.; Toledo, J.; Srivastava, S. Structure of Nanoparticle-Polyelectrolyte Complexes: Effects of Polyelectrolyte Characteristics and Charge Ratio. *AIChE Journal* **2021,** *67*, e17443.
31. Tiraferri, A.; Maroni, P. Rapid Desorption of Polyelectrolytes from Solid Surfaces Induced by Changes of Aqueous Chemistry. *Langmuir* **2018,** *34*, 12302-12309.
32. Klačić, T.; Katić, J.; Namjesnik, D.; Jukić, J.; Kovačević, D.; Begović, T. Adsorption of Polyions on Flat TiO_2 Surface. *Minerals* **2021,** *11*, 1164.
33. Popa, I.; Cahill, B. P.; Maroni, P.; Papastavrou, G.; Borkovec, M. Thin Adsorbed Films of a Strong Cationic Polyelectrolyte on Silica Substrates. *Journal of Colloid and Interface Science* **2007,** *309*, 28-35.
34. Sáringer, S.; Rouster, P.; Szilágyi, I. Regulation of the Stability of Titania Nanosheet Dispersions with Oppositely and Like-Charged Polyelectrolytes. *Langmuir* **2019,** *35*, 4986-4994.
35. Hoogeveen, N. G. C. S., M. A.; Fleer, G. J. Polyelectrolyte Adsorption on Oxides II. Reversibility and Exchange. *J. Colloid Interface Sci.* **1996,** *182*, 146-157.
36. Kleijn, J. M.; Barten, D.; Cohen Stuart, M. A. Adsorption of Charged Macromolecules at a Gold Electrode. *Langmuir* **2004,** *20*, 9703-9713.
37. Rojas, O. J.; Ernstsson, M.; Neuman, R. D.; Claesson, P. M. Effect of Polyelectrolyte Charge Density on the Adsorption and Desorption Behavior on Mica. *Langmuir* **2002,** *18*, 1604-1612.

38. Koumarianos, S.; Kaiyum, R.; Barrett, C. J.; Madras, N.; Mermut, O. Theory and Experiment of Chain Length Effects on the Adsorption of Polyelectrolytes onto Spherical Particles: The Long and the Short of It. *Phys. Chem. Chem. Phys.* **2021,** *23*, 300-310.
39. Mészáros, R.; Varga, I.; Gilányi, T. Adsorption of Poly(Ethyleneimine) on Silica Surfaces - Effect of Ph on the Reversibility of Adsorption. *Langmuir* **2004,** *20*, 5026-5029.
40. Fu, J.; Fares, H. M.; Schlenoff, J. B. Ion-Pairing Strength in Polyelectrolyte Complexes. *Macromolecules* **2017,** *50*, 1066-1074.
41. Fleer, G.; Cohen Stuart, M.; Scheutjens, J. M.; Cosgrove, T.; Vincent, B. *Polymers at Interfaces*; Springer Science 1993.
42. Xie, F.; Lu, H.; Nylander, T.; Wågberg, L.; Forsman, J. Theoretical and Experimental Investigations of Polyelectrolyte Adsorption Dependence on Molecular Weight. *Langmuir* **2016,** *32*, 5721-5730.
43. Bayari, S.; Yurdakul, Ş. Fourier Transform Infrared and Raman Spectra of 4-Vinylpyridine and Its Transition Metal(II) Tetracyanonickelate Complexes. *Spectroscopy Letters* **2000,** *33*, 475-483.
44. Eisenberg, A.; Gauthier, S.; Duchesne, D. Vinylpyridinium Ionomers. 1. Influence of the Structure of the Ion on the State of Aggregation in Random Styrene-Based Systems. *Macromolecules* **1987,** *20*, 753-759.
45. Schlenoff, J. B.; Yang, M.; Digby, Z. A.; Wang, Q. Ion Content of Polyelectrolyte Complex Coacervates and the Donnan Equilibrium. *Macromolecules* **2019,** *52*, 9149-9159.
46. Bucur, C. B.; Sui, Z.; Schlenoff, J. B. Ideal Mixing in Polyelectrolyte Complexes and Multilayers: Entropy Driven Assembly. *Journal of the American Chemical Society* **2006,** *128*, 13690-13691.
47. Henzler, K.; Haupt, B.; Lauterbach, K.; Wittemann, A.; Borisov, O.; Ballauff, M. Adsorption of β-Lactoglobulin on Spherical Polyelectrolyte Brushes: Direct Proof of Counterion Release by Isothermal Titration Calorimetry. *Journal of the American Chemical Society* **2010,** *132*, 3159-3163.
48. Nakatani, A. I.; Mohler, C. E.; Hughes, S. Chain Conformation of Polymers Adsorbed to Clay Particles: Effects of Charge and Concentration. *Soft Matter* **2021,** *17*, 6848-6862.
49. Dugger, D. L.; Stanton, J. H.; Irby, B. N.; McConnell, B. L.; Cummings, W. W.; Maatman, R. W. The Exchange of Twenty Metal Ions with the Weakly Acidic Silanol Group of Silica Gel. *The Journal of Physical Chemistry* **1964,** *68*, 757-760.
50. Lunkad, R.; Fernando, L.; Silver, B.; Peter, K. Both Charge-Regulation and Charge-Patch Distribution Can Drive Adsorption on the Wrong Side of the Isoelectric Point. *Journal of the American Society.* **2022,** *144*, 1813-1825.
51. Shubin, V.; Linse, P. Self-Consistent-Field Modeling of Polyelectrolyte Adsorption on Charge-Regulating Surfaces. *Macromolecules* **1997,** *30*, 5944-5952.
52. Hernández-Rivas, M.; Guzmán, E.; Fernández-Peña, L.; Akanno, A.; Greaves, A.; Léonforte, F.; Ortega, F.; G. Rubio, R.; Luengo, G. S. Deposition of Synthetic and Bio-Based Polycations onto Negatively Charged Solid Surfaces: Effect of the Polymer Cationicity, Ionic Strength, and the Addition of an Anionic Surfactant. *Colloids and Interfaces* **2020,** *4*, 33.
53. Sedeva, I. G.; Fornasiero, D.; Ralston, J.; Beattie, D. A. The Influence of Surface Hydrophobicity on Polyacrylamide Adsorption. *Langmuir* **2009,** *25*, 4514-4521.
54. Balzer, C.; Jiang, J.; Marson, R. L.; Ginzburg, V. V.; Wang, Z. G. Nonelectrostatic Adsorption of Polyelectrolytes and Mediated Interactions between Solid Surfaces. *Langmuir* **2021,** *37*, 5483-5493.

55. Greene, B. W. The Effect of Added Salt on the Adsorbability of a Synthetic Polyelectrolyte. *Journal of Colloid and Interface Science* **1971,** *37*, 144-153.
56. Christensen, J. J.; Oscarson, J. L.; Izatt, R. M. Thermodynamics of Proton Ionization in Dilute Aqueous Solution. X. ΔG (pK), ΔH, and S Values for Proton Ionization from Several Monosubstituted Carboxylic Acids at 10, 25, and 40 Degrees. *Journal of the American Chemical Society* **1968,** *90*, 5949-5953.
57. Barbucci, R.; Paoletti, P.; Vacca, A. Predictions of the Enthalpies of Protonation of Amines. Log K, ΔH, and ΔS Values for the Protonation of Ethylenediamine and Tri-, Tetra-, Penta-, and Hexa-Methylenediamine. *Journal of the Chemical Society A* **1970**, 2202-2206.
58. Lunkad, R.; Murmiliuk, A.; Hebbeker, P.; Boublík, M.; Tošner, Z.; Štěpánek, M.; Košovan, P. Quantitative Prediction of Charge Regulation in Oligopeptides. *Molecular Systems Design & Engineering* **2021,** *6*, 122-131.
59. Dange, C.; Phan, T. N. T.; André, V.; Rieger, J.; Persello, J.; Foissy, A. Adsorption Mechanism and Dispersion Efficiency of Three Anionic Additives [Poly(Acrylic Acid), Poly(Styrene Sulfonate) and HEDP] on Zinc Oxide. *Journal of Colloid and Interface Science* **2007,** *315*, 107-115.
60. DeRosa, R. L.; Schader, P. A.; Shelby, J. E. Hydrophilic Nature of Silicate Glass Surfaces as a Function of Exposure Condition. *Journal of Non-Crystalline Solids* **2003,** *331*, 32-40.
61. Ueda, T.; Harada, S. Adsorption of Cationic Polysulfone on Bentonite. *Journal of Applied Polymer Science* **1968,** *12*, 2395-2401.
62. Al Mahrouqi, D.; Vinogradov, J.; Jackson, M. D. Zeta Potential of Artificial and Natural Calcite in Aqueous Solution. *Advances in Colloid and Interface Science* **2017,** *240*, 60-76.
63. Portnov, I. V.; Potemkin, I. I. Interpolyelectrolyte Complex Dissociation Vs Polyelectrolyte Desorption from Oppositely Charged Surface Upon Salt Addition. *The Journal of Physical Chemistry B* **2020,** *124*, 914-920.
64. Yang, M.; Sonawane, S. L.; Digby, Z. A.; Park, J. G.; Schlenoff, J. B. Influence of "Hydrophobicity" on the Composition and Dynamics of Polyelectrolyte Complex Coacervates. *Macromolecules* **2022,** *55*, 7594-7604.
65. Schrader, A. M.; Monroe, J. I.; Sheil, R.; Dobbs, H. A.; Keller, T. J.; Li, Y.; Jain, S.; Shell, M. S.; Israelachvili, J. N.; Han, S. Surface Chemical Heterogeneity Modulates Silica Surface Hydration. *Proceedings of the National Academy of Sciences* **2018,** *115*, 2890-2895.
66. Lagström, T.; Gmür, T. A.; Quaroni, L.; Goel, A.; Brown, M. A. Surface Vibrational Structure of Colloidal Silica and Its Direct Correlation with Surface Charge Density. *Langmuir* **2015,** *31*, 3621-3626.
67. Dalstein, L.; Potapova, E.; Tyrode, E. The Elusive Silica/Water Interface: Isolated Silanols under Water as Revealed by Vibrational Sum Frequency Spectroscopy. *Physical Chemistry Chemical Physics* **2017,** *19*, 10343-10349.
68. Kodama, H.; Miyajima, T.; Mori, M.; Takahashi, M.; Nishimura, H.; Ishiguro, S. A Unified Analytical Treatment of the Acid-Dissociation Equilibria of Weakly Acidic Linear Polyelectrolytes and the Conjugate Acids of Weakly Basic Linear Polyelectrolytes. *Colloid and Polymer Science* **1997,** *275*, 938-945.
69. Hansupalak, N.; Santore, M. M. Polyelectrolyte Desorption and Exchange Dynamics near the Sharp Adsorption Transition: Weakly Charged Chains. *Macromolecules* **2004,** *37*, 1621-1629.

70. Vermöhlen, K.; Lewandowski, H.; Narres, H. D.; Schwuger, M. J. Adsorption of Polyelectrolytes onto Oxides — the Influence of Ionic Strength, Molar Mass and Ca^{2+} Ions. *Colloids and Surfaces A* **2000,** *163*, 45-53.
71. Böhmer, M. R.; Evers, O. A.; Scheutjens, J. M. M. Weak Polyelectrolytes between Two Surfaces - Adsorption and Stabilization. *Macromolecules* **1990,** *23*, 2288-2301.